

The use of JERS-1 data for environment modeling, resources assessment and deforestation detection in Amazônia.

Luciano Vieira Dutra, João Roberto dos Santos, Corina da Costa Freitas, Evlyn Moraes de Leão Novo, Diógenes Salas Alves, Pedro Hernandez Filho.

Instituto Nacional de Pesquisas Espaciais. INPE,
12.227-010 Av. dos Astronautas, 1758 - J. Granja,
São José dos Campos, SP - BRAZIL
Caixa Postal (P.O. Box) 515, 12201-970
Tel. + 55-12-3945 6444 -Fax:+55-12-3945 6468,
e_mail: dutra@dpi.inpe.br

Abstract

This paper presents an updated report of the Brazilian experience on the use of JERS-1 data as an information source for biomass estimation, land use / land cover characterization and delineation of different habitats in Amazônia. Primary and secondary forest and savanna biomass measurements were acquired in Acre and Roraima, respectively, and their values were related to JERS-1 backscatter. JERS-1 texture was used to improve land cover mapping accuracy in Tapajós, (Pará State) and the State of Rondônia. Floodplain habitats were mapped in Monte Alegre Lake (northeast of Brazilian Amazônia) with the joint use of JERS-1 and Radarsat images. Also the use of JERS_1 to detect deforestation, and a comparison with operational methods, is discussed

1 Introduction.

Key questions in Amazonian studies are: how do deforested areas evolve? How differences on biomass can affect carbon budget? How to classify different types of primary forest? Different types of forest have different potentials for sustainable exploitation. Biomass estimation for different Amazonian communities is a piece of the carbon balance related to changes in tropical environments. Mapping the different habitats in Amazon is very important towards the comprehension of such rich ecosystem. Remote Sensing is the necessary tool to use given the dimension of Amazon region, and particularly the use of SAR data, considering its complementary characteristics with optical data and cloud free acquisition.

The Brazilian Space Research Institute (INPE) has been working on several aspects of the mentioned problems and this report focuses on some results based on JERS-1 data on the fields of biomass estimation (section 2), land cover characterization and delineation of different habitats in Amazon (section 3).

Distinct methodologies and different aspects of Amazonian landscapes are discussed in the following sections. It is expected that these discussions may lead to a better understanding of the Amazonian environment and to an adequate evaluation of available and new methodologies that are necessary for monitoring this important ecosystem.

2 Relationship between backscattering and biomass estimates.

The spatial distribution of the tropical rain forest and savanna formation biomass for the entire Amazon region is a fundamental information to the understanding of global change processes. The relationship between biophysical parameters of vegetation cover and backscattering derived from JERS-1 image was examined for two test sites. Alto Alegre test site (Roraima State) represents a sharp boundary between forest and savanna formations (Santos et al., 1998b) and Rio Branco test site (Acre State) is an area of dense/open tropical rain forest (Santos et al., 1998a).

In both test sites, the linear spectral mixture model was applied to TM/Landsat scenes to create a reference database for land cover classes discrimination and to locate sample sites for ground data

collection. These TM/Landsat images were registered to the JERS-1 scenes with a geometric accuracy of one pixel to derive σ^0 values (dB) from previously selected sample areas. The backscatter coefficient was derived from digital numbers as follows (Rosenqvist, 1997):

$$\sigma^0 = 10 \log_{10} \{(\Sigma DN^2) / n\} + CF$$

where DN = digital number of the amplitude image pixel; n = number of pixels of the sample area and CF = offset calibration factor (-68.5 dB).

Two procedures for data collection were used. In the savanna, biomass estimation of the herbaceous, bush and shrub vegetation was measured by cutting and weighting them in samples with size ranging from 200 to 500m², according to the savanna physiognomy. At each sample all individuals of bush and/or arboreal strata were botanically identified and weighted. For the herbaceous strata, biomass and percentage soil coverage was estimated in at least five sections with 1m² size each. In forest areas the following measurements were made: DBH, height, crown cover percentage, as well as the botanical identification of all individuals with DBH > 5cm for secondary succession and DBH > 10cm for primary forest, at sample areas of 1,000m² and 2,500m² respectively (Figure 1). The estimation of biomass values was modeled by dendrometric parameters into the allometric equations. Statistical procedures, using simple or multiple regression models were used to estimate the relationship between field data (biomass

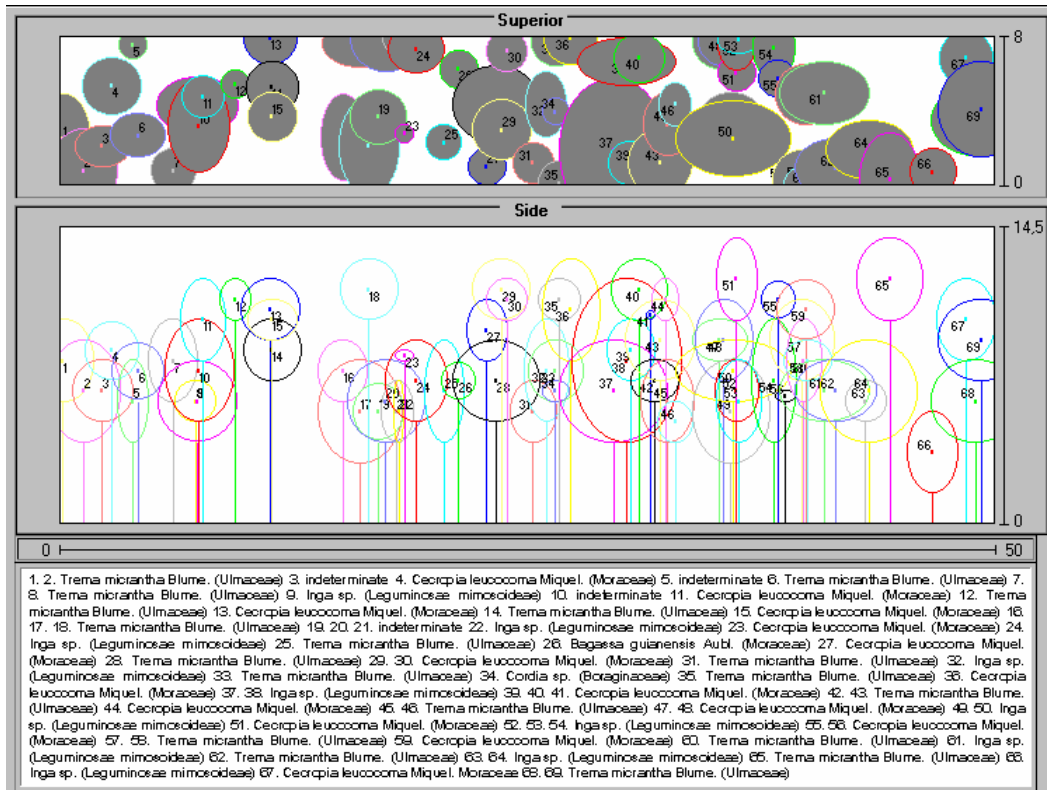


Figure 1 - Example of typical physiognomic profile of an intermediate secondary succession. Source: Santos et al.(1998b).

values) and those obtained from orbital images.

The following land cover classes were identified: primary forest, intermediate secondary succession, savanna grassland, parkland savanna and savanna woodland (Santos et al., 1998a). The mean biomass values obtained for primary and secondary forest was around 194.71 ton/ha and 47.06 ton/ha (dry weight) respectively. Secondary succession samples presented 20% biomass related to the vegetation development degree and to the intensity of previous usage. Primary forest (DBH > 10cm) presented an average of 430 individuals/ha, DBH of 23.60cm and average canopy height of 14.54m (the highest individuals are up to 38m height). Secondary succession (DBH > 5cm) presented, in average, 1294

individuals/ha, DBH around 11.22cm, and height around 7.94m. In savanna formations, the estimated biomass (dry weight) was: 4.86 ton/ha for savanna grassland, 7.28 ton/ha for parkland savanna, and 20.15 ton/ha for savanna woodland. The savanna grassland has just the herbaceous stratum, formed by graminea species and cyperaceae, presenting in average 48.57% of soil coverage. The parkland savanna presented 230 individuals/ha at the upper stratum (bush and small trees) which represented 40% of the whole biomass. These values are different for savanna woodland, where 82% of the biomass belongs to the arboreal/bush stratum, showing an average of 300 individuals/ha.

The estimated relationship between the backscatter values from JERS-1 and biomass indicators (Figure 2) is shown in Figure 2. In the simple regression model, biomass values were considered as independent variable (x) and the estimated equation $y = 1.7881 \ln(x) - 15.821$ had a coefficient of determination $r^2 = 0.8746$. The range of backscatter values varied from -9.04 to -5.77 dB for forestry formations and from -15.07 to -9.55 dB for savanna types. It could be observed that this regression function shows a high sensitiveness to biomass up to 100 ton/ha. The components of “vegetation”, “soil” and “shade” are related to the variability of the vegetation structure and soil moisture content and are responsible for changes in the backscatter signal.

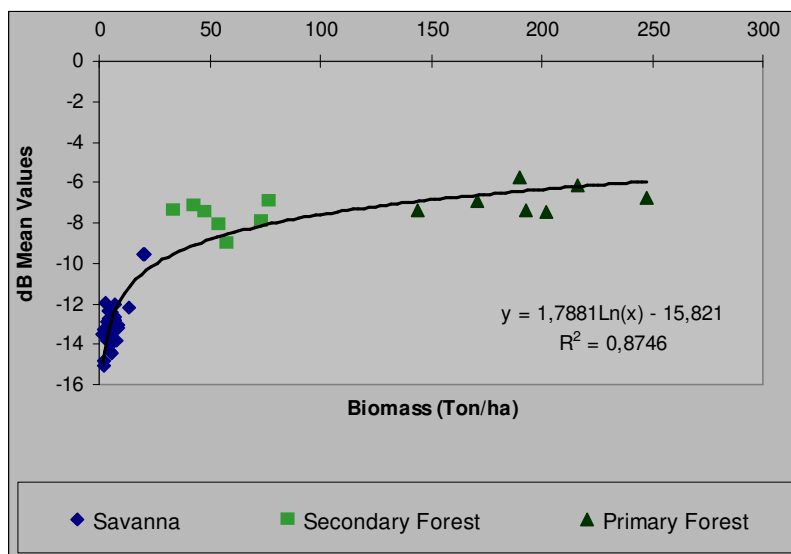


Figure 2 - Diagram of JERS-1 backscatter values of forest and savanna formations. Source: modified from Santos et al. (1998b).

In the Acre test site the integration of TM-Landsat and Jers-1 images allowed to identify primary rain forest with or without bamboo species (*Guadua weberbaueri* Pilger) and different levels at secondary succession (Santos et al., 1998b). Primary forest with high proportions of “vegetation” and “shade” displayed backscatter coefficient between -7 to -6 dB. The different stages of secondary succession are defined on the -7.8 to -10.4 dB range. This range is affected by changes in the physiognomic-structural characteristics and by species composition of the natural vegetation regrowth. The biomass content was estimated from a multiple regression model (determination coefficient $r^2 = 0.77$ and standard error of the estimate $S_{xy} = 32.64$) derived from JERS-1 backscatter and TM/Landsat spectral information. The model was sensitive to biomass values up to 90 ton/ha.

3 Feature extraction for land use/ land covers classification.

Texture is an important feature to use SAR imagery for digital classification purposes. Several methods have been presented in the literature with limited success. Most of them rely on a filtering process over the original image, in which the texture information around a certain pixel position is extracted considering a determined neighborhood of that pixel. This texture information is assigned to the pixel position, which is the center of its neighborhood, and it is used as a component of a feature vector that will be used in pixel based classifier. Important issues are 1) filter size used to extract the texture information and 2) the underlying texture model.

Haralick's texture features (Haralick et al., 1973), also known as co-occurrence features, are widely used. Here is presented a study to determine a convenient size of neighborhood for Haralick's feature extraction (section 3.1); a study which consider the joint use of co-occurrence features with features extracted by matched filtering(section 3.2) and an assessment of a region classifier based on Haralick's features, local statistics, distribution parameters and autocorrelation function derived features (section 3.4) for land use / land cover classification using JERS-1 imagery. In section 3.3, a texture feature extraction method based on autorregressive modeling is presented for primary forest classification as observed by JERS-1 imagery.

3.1 Use of texture measures for detection of tropical deforestation.

The potential of using texture features for mapping land cover classes as seen in JERS-1 imagery were investigated for a test site in Rondônia (Ribeiro *et al.*, 1998). Sixty-nine control plots were defined in the test area and their land cover classes were established from site visits, aerial and TM/Landsat imagery. Land covers classes under consideration were recent deforestation (RD); pasture or bare soil (PA); young secondary forest (Y2F); intermediate secondary forest (I2F); old secondary forest (O2F), and mature forest (MF).

An analysis of the performance of 14 texture measurements (Haralick; 1979) was performed, by calculating texture-images of mean (mean); vari (variance); ener (energy); corr (correlation); entr (entropy); cont (contrast); homo (local homogeneity); diss (dissimilarity); smea (mean of sum vector); svar (variance of sum vector); sent (entropy of sum vector); dmea (mean of difference vector); dvar (variance of difference vector) and dent (entropy of difference vector). All texture images were normalized to have zero mean and unitary standard deviation. Window sizes of 5x5, 7x7, 9x9, 11x11, and 15x15-pixels were investigated. The Mahalanobis distance (D2), as described in Schowengerdt (1997), were computed for all texture measurements and window sizes, for fifteen pair-wise combination of the land cover classes (RD-PA; RD-Y2F; PA-MF etc). The 11x11-pixels window was selected by maximizing the Mahalanobis distance. Figure 3a presents the D2 values for the RD-PA pair. The plots for other pairs, not showed here, presented similar results.

Calculating the Mahalanobis distance between all pairs of the land cover classes, showed that texture measures - mean, variance, entropy, contrast, local homogeneity, and mean of sum vector - allowed to maximize inter-class distances and discriminate between several land cover classes (Figure 3b), particularly between mature forest (MF) and pasture (PA), and forest and recent deforestation (RD). It was also possible to observe, from Figure 3b, that entropy (entr) was the best one to discriminate recent deforestation (RD) from all other classes, mean of sum vector(smea) and mean provided a very good separation between RD and pasture (PA). Discrimination between mature forest (MF) and older stages of secondary growth (I2F, O2F) revealed to be more difficult. In general, the choice of which feature will be the best for pair-wise land cover class discrimination will depend on that particular class pair.

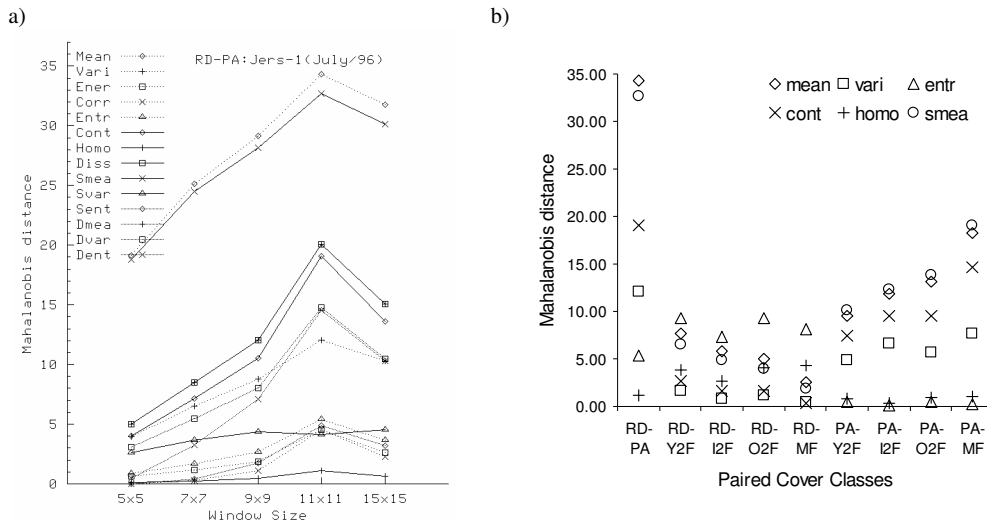


Figure 3 - Mahalanobis distances between paired cover classes: a) window size analysis for RD-PA classes; b) best texture measurements using 11x11 filter size. Source: modified from Ribeiro *et al.* (1998).

3.2 Feature extraction by local statistics, co-occurrence and matched filters.

Recent studies based on visual interpretation and usage of established classification techniques exhibited weaknesses concerning correct classification of all classes of interest in Amazônia, particularly different types of primary forest, when using radar data. Sometimes only forest-non forest discrimination is possible. Image texture is a key factor to discriminate primary forests, while L- band backscatter has the ability to discriminate forest from non-forest.

In this study, 11 classes of general interest could be established near and inside the Tapajós National Forest, which is located south of city of Santarém, Pará State, Brazil. The classes defined for analysis are: 1) dense forest – dissected plateau (DFDP); 2) dense forest – high plateau (DFHP); 3) urban areas; 4) open forest (OF); 5) dense forest – sedimentary area (DFSA); 6) mature regeneration; 7) pasture; 8) bare soil; 9) abandoned (dirt) pasture; 10) water; 11) aquatic vegetation. It was used the scenes 405/306 and 405/307 (acquired Aug 13, 1996). Figure 4 presents a mosaic of samples of these classes. From this mosaic 28 texture feature images were extracted by specialized filtering determined for each texture model. Such a large number of features were chosen with hope of discriminating as many classes as possible. Even with such a large number of features it is expected that some classes can not be discriminated. The objective here is to develop an analysis methodology to discover which are the best features from the set, considering the classes of interest, and which classes cannot be well discriminated even with the best set composition.

The methodology can be summarized as follows: 1) extraction of 28 feature images; 2) selection of 11 features using 2 discrimination ranking coefficients (Huber and Dutra, 1998) based on average Jeffries-Matusita distance (JMD) (Fukunaga, 1990) for the classes; 3) grouping and renaming of not separable classes using a closeness threshold (by JMD); 4) assessment of the discrimination power of all possible subsets of 11 features by evaluating the classifier performance on those subsets. The best subset was chosen as the one with higher overall accuracy.

The texture features used (Dutra *et al.*, 1998) were: 7 types of local statistics filter, 10 types of co-occurrence features and 11 output variance of matched filters to the classes textures. Matched filters are constructed by a linear composition of Laws (1980) filters as described in (Dutra *et al.*, 1998).

Ranking coefficients was used to pre-select features, because using exhaustive search with 28 features is not feasible. Also, the JMD between all pair of classes, for the chosen 11 features set, is used to build a graph linking all classes by minimum distance. This graph permits to identify classes which are not considered statistically separable by setting a minimum JMD to leave neighboring classes in the graph apart.

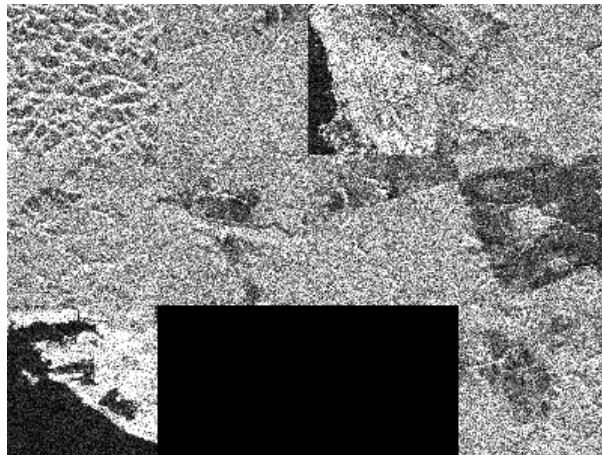


Figure 4 - Mosaic with samples of JERS-1 scenes containing 11 classes of interest.

Source: Dutra et al. (1998)

Considering a threshold of 0.7, a new set of classes was obtained: 1) DFDP; 2) flat forest (FF) which is composed by DFHP, OF, DFSA and mature regeneration; 3) urban areas; 4) pasture + bare soil; 5) abandoned (dirt) pasture; 6) water and 7) aquatic vegetation.

Each possible subset of features from the set with 11 features was used to train an one hidden layer multilayer perceptron (MLP) classifier by resilient back-propagation (RPROP) method and considering the new set of seven classes. The subset with the higher overall accuracy calculated on a validation set is selected. Training and validation sets are composed by 500 randomly chosen points per class. The best subset of features is composed by eight features: the original backscatter; coefficient of variation for intensity, entropy; contrast; homogeneity and three matched filters output variance of classes DFDP; urban areas and bare soil.

Table 1 presents the overall accuracy together with Tau coefficient of agreement (Ma et al., 1995) considering the classification result using the best features subset and classifying into the seven grouped classes. For comparison the MLP classifier was trained on basic features, e.g. filtered backscatter image and intensity coefficient of variation, using the same training samples. See first column of Table 1. Figure 5 shows the result of contextual MLP classification, which is an improvement of the MLP classifier as described in Dutra et al. (1998).

Table 1: Classifier Performance for MLP (%).

Validation Sets	Basic Features	Best Subset	Best Subset + Context
Overall Accuracy	53.7	80.2	86.5
Tau	45.6	76.9	84.2

Source: Dutra et al. (1998).

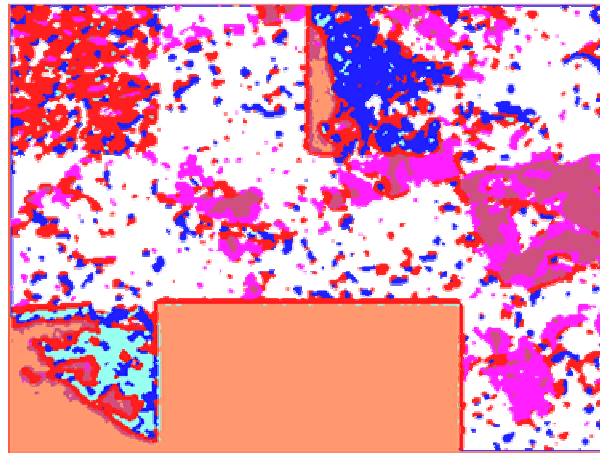


Figure 5 - MLP contextual classification result. Source: Dutra et al. (1998).

As shown in the results, texture feature extraction plays an important role in land use classification when using JERS-1 imagery. Particularly, feature extraction from matched filtering allowed a better discrimination of dense forest of dissected plateau, which normally would be confused with most classes because its undulated relief.

3.3 Feature extraction by autoregressive modeling.

A texture feature extraction method using autoregressive modeling was developed and tested for rain forest classification using JERS-1 SAR image from Tapajós National Forest, Pará State, Brazil.

The Autoregressive (AR) models assume time series as being generated by a linear filter (Figure 6) excited by a white noise. The input of this filter, called *shocks*, is a time sequence of independent random variables, identically distributed with null average and variance σ^2 , IID(0, σ^2). The output of this filter Z_t is given by equation 1.



Figure 6 - Time serie Z_t as output of linear filter, excited by white noise a_t .

Source: Soares et al. (1998).

$$Z_t = \sum_{k=1}^p \phi_k \cdot Z_{t-k} + a_t + \mu \quad \text{or} \quad (1a)$$

$$Z_t^* = \phi_1 \cdot Z_{t-1}^* + \dots + \phi_p \cdot Z_{t-p}^* + a_t \quad (1b)$$

where $Z_t^* = Z_t - \mu$.

The parameters ϕ_k , in the equations 1a and 1b, can be estimated by the Yule-Walker equations, using the recursive Levinson-Durbin algorithm, as described in Kay (1988).

An extension for the two-dimensional case was used as described in Dutra (1990). The methodology for feature extraction and classification can summarized by the following steps:

- Stage 1 - Autoregressive Model Estimation: a model is estimated for each textural class;
- Stage 2 - Definition of Autoregressive Inverse Filters: inverse filters are derived from each AR model by calculating an estimate for a_t as a function of Z_t (Equation 1) and its past values for each set of autoregressive parameters, which was estimated for each textural class;
- Stage 3 - Inverse AR Filtering, Whitening and Energy: matched inverse autoregressive filters, relative to each class, are applied sequentially to the original image producing an estimate of the shocks (called residues) as seen by each inverse filter. For each residues channel the energy and whitening coefficient channels are calculated as indicate in Soares (1998). When a region is filtered by its matched correspondent filter, the resulting field is expected to yield minimum energy when compared to all other non matched filters and the whitening coefficient channels approximates zero (Soares, 1998).

As a result, a set of M bands of filtered images, where M is equal of number of classes multiplied by three, are obtained from the original image:

- The raw output of the inverse filters;
- The whitening coefficient images calculated from the outputs of the inverse filters;
- The energy bands, also calculated from the outputs of the inverse filters.

- Stage 4 - Maximum Likelihood Classification: the set of filtered bands of the original image is then classified by the Maximum Likelihood classifier with the same training samples that had generated the AR parameters (Soares, 1998).

To test the method, a mosaic of JERS-1 sub-images containing representative textures of two types of forest: dense flat forest and undulated (dissected) forest was chosen. The mosaic (Figure 6) is composed by JERS-1 sample areas from Tapajós National Forest (Pará State, Brazil).

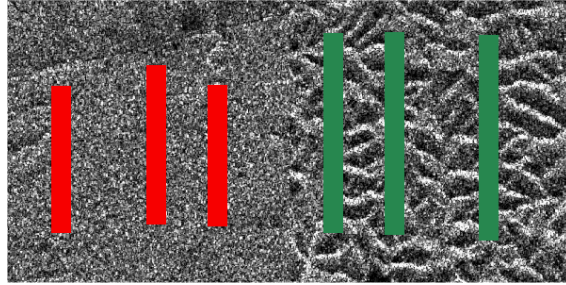


Figure 6 - Mosaic of JERS-1 images with dense flat forest (right) and undulated forest (left) The training areas are shown in red and green for flat forest and undulated forest. Source: Soares et al. (1998).

Applying the maximum likelihood classification to the six band set, the result of Figure 7 was produced.



Figure 7 - Classification on the set of all the bands generated in the stage-4. Source: Soares et al. (1998).

The results were analyzed using the confusion matrix, and showed a Kappa coefficient of 96.1%, instead of a Kappa of 36.1% using the original channel only for classification, whose result is shown in Figure 8.

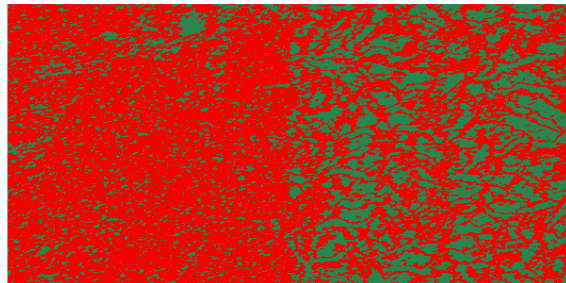


Figure 8 - Maximum Likelihood Classification of the single channel original JERS-1 Mosaic. Source: Soares et al. (1998).

3.4 Region classifier based on textural features.

In this section, a classification of a JERS-1 image from the Tapajós region (Pará State, Brazil) is presented. The classes of interest are: primary forest, old secondary forest, new secondary forest and recent activities (bare soil, pasture and crops) In order to perform the classification, a system over IDL/ENVI environment was developed and implemented (Rennó et al., 1998). It consists on the three main stages (modules): analysis and selection of textural features and classification. The selected features are used as discriminant attributes by a supervised region classifier. More than one hundred textural features were implemented in this system, split on four groups: local statistics (seven), distributional (eight), Haralick's (eighteen) and autocorrelation (can be calculated from lags -4 to 4, and also ratios between two of them).

The first set includes measures of local statistics as skewness, kurtosis, coefficient of variation and median, among others. The distributional measures are parameters of statistical distributions, some of

them specific for radar data. The reader interested in more details about the distributions used to model radar data is recommended to Frery et al. (1997) and the references within it. The measures found in both groups are calculated without considering spatial distribution of pixels. The Haralick's measures set is based on the Gray Level Co-occurrence Matrix (GLCM). The GLCM describes the frequencies of the co-occurrence of two specific gray-levels given specific pixel locations in terms of relative direction and distance (Haralick, 1979). The dissimilarity, energy, homogeneity, cluster shade and cluster prominence are some measures that can be found in this set.

It is evident that a large number of measures can be extracted and become impracticable to use all of them in the image classification step. The used decision rule to choose one or more measures is based on a discriminant factor, which is estimated from training samples. This discriminant factor evaluates the separability between classes, considering the variation within and between two classes. The last phase is the classification, which classify each region, from a previously segmented image, minimizing the Mahalanobis distance. In this work the segmented image was obtained from a landuse map built using a multitemporal series of TM/Landsat images (Sant'Anna et al., 1995).

The classification was obtained in two steps (tree classifier): the first consisted on classifying groups of classes with similar characteristics and the second on classifying, for each group, the grouped classes. The result was obtained by using the median measure to separate the group formed by primary forest and old secondary forest classes from the group formed by new secondary forest and recent activities classes. The Haralick's entropy measure was utilized to distinguish the former group, and the later one was separated by median measure. This result might be considered good because of the areas of old secondary forest, which present characteristics very similar to primary forest, were well classified.

Figure 9 shows the JERS-1 image from 06/26/93 and the result of classification when two steps were used. The classified image presents four classes: primary forest, old secondary forest, new secondary forest and recent activities, colored by dark green, light green, yellow and magenta, respectively.

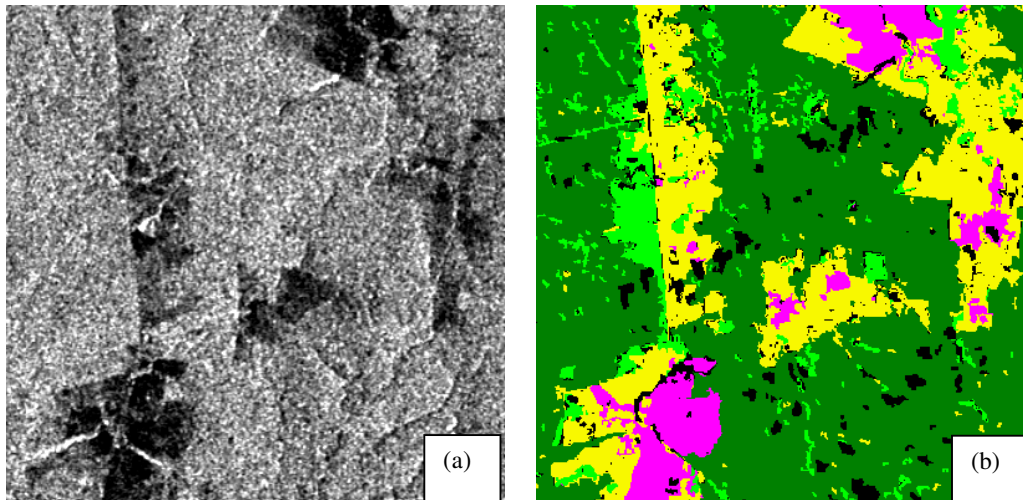


Figure 9 - (a) JERS-1 image and (b) Classification based on median and Haralick's entropy measures performed in two steps. Source: modified from Rennó et al. (1998).

4 Application of region growing segmentation method for floodplain habitats delineation.

The study was carried out in Monte Alegre lake ($2^{\circ}10'S/54^{\circ}20'W$) in the northeast of the Brazilian Amazon as reported by Costa et al., (1997). In this study multisensor (JERS-1 and Radarsat) image data set was used to map floodplain habitats using a region growing segmentation method.

The data set for the study consisted of aerial photography, Radarsat and JERS-1 images and field observations such as hand-help photographs, collected GPS coordinates and field description of the test site. The color aerial photographs were acquired at 1:20,000 scale at the end of May, 1996. They were

scanned, mosaicked, visually interpreted and subsequently digitized for creating a digital land cover map. The resultant map was used as a ground truth map. Three Radarsat standard mode images acquired in May (S1 and S6) and August (S6) and two JERS-1 images acquired in May and July were used to map the following ground classes: Water, Forest, Flooded Forest, Aquatic plants, Pasture.

The images were ortho-rectified according to the methodology developed by Toutin, (1995). The accuracy of the model was on average 11.4m, the accuracy of the restitution was on average 19.2m, and the final resolution was 12.5m. Detailed information about the images ortho-correction are reported by Costa et al., 1997. A subscene (20 x 20km) near Maicurú river was selected and submitted to the following procedures: a) linear scaling from 16 to 8 bit; b) speckle filtering with Lee Filter (7 x 7 window) (Lee, 1981); c) segmentation using a region growing algorithm; d) supervised classification of the pre-segmented image using a Bhattacharyya distance algorithm; e) class area estimation. Different threshold combination was tested, either for single data or for a combination of both, Radarsat and JERS-1. Figure 10 shows a segmentation of a Radarsat S6 and a JERS-1, both acquired in May and Figure 11 shows the radar color composition.

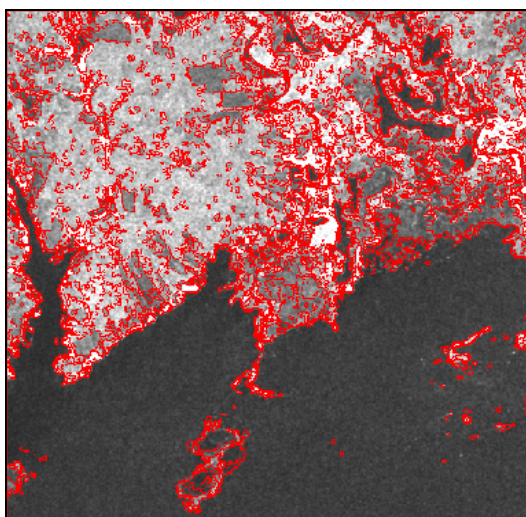


Figure 10 – Segmentation of Radarsat S6 and JERS-1, May. Source: Costa et al. (1997).

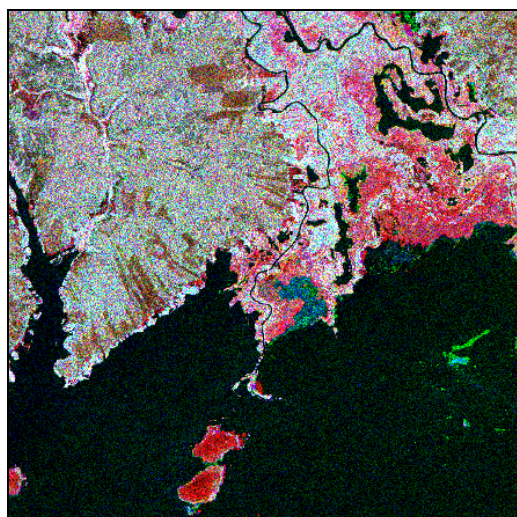


Figure 11 - Color composite, Radarsat S6 May (red), JERS-1 May (green) and JERS-1 August (blue). Source: Costa et al. (1997).

Table 2 summarizes the calculated area for each classified class. The ground truth map data has an extra class (no-data), which represents lack of information related to cloud cover in the area. To overcome this lack of information the ground truth map was compared with the images and the “no-data” class was then associated to the real classes. Therefore, it must be considered that the no-data area generated from the ground truth map corresponds, at least, to approximately 80 km² of water, 20 km² of forest and the remaining area (18.4 km²) could be part of flooded-forest, pasture and aquatic-plants classes. The parenthesis values in Table 2 correspond to the area values for the ground truth map data assuming spatial continuity of the ground class as displayed in the radar data set. The ground truth map classes followed by an interrogation mark are those where the spatial continuity assumption do not hold thoroughly.

Table 2. Calculated area for the classified data (km²).

	Water	Forest	Flooded-forest	Aquatic-plants	Pasture	no data
Ground truth map	82.4 (162.4)	43.6 (63.6)	33.0 (?)	41.3 (?)	28.5 (?)	118.4
JM	167.9	72.9	24.6	43.1	42.55	
RS6M	164.4	77.8	21.1	64.2	23.5	
RS6MJM	159.9	78.72	31.1	57.35	23.9	
JJ	166.9	71.5	31.5	44.0	37.1	
RS6A	169.1	71.1	16.9	61.3	32.9	
RS6AJJ	168.46	70.0	27.5	53.3	31.7	
RS1M	164.86	85.2	36.9	43.2	20.8	
RS1MJM	165.8	72.1	29.8	56.6	26.7	

JM= JERS-1 May - Source: Costa et al., 1997.

RS6M = Radarsat Standard mode beam 6, May
RS6MJM= both JM and RS6M used to run the classification
JJ= JERS-1 image, June
RS6A = Radarsat Standard mode beam 6, August
RS6AJJ= both JJ and RS6A used to run the classification
RS1M= Radarsat Standard mode beam 1, May
RS1MJM= both JM and RS1M used to run the classification

It was observed an improved classification when JERS-1 and Radarsat are used in combination when compared with the digital ground truth map. The reasons for that are the distinct incidence angle, wavelength and date.

5 Conclusions.

Although is not possible to consider the results shown as definitive, certain conclusions can be drawn:

1. There exists a relationship between the radar backscatter and biomass for the contact zone of forest and savanna formation. The sensitiveness of this relationship is quite high for biomass values up to about 100 ton/ha.
2. Texture is a very important feature for improving classification accuracy but, in general, is not possible to point out a specific texture model as the best for all cases.
3. Co-occurrence texture features can be used successfully either for per point or region classification.
4. The results suggest that better results are obtained using different texture models at the same time and employing a feature selection routine to seek the best features according the set of classes of interest.
5. The use of texture permitted the discrimination of old secondary forest from primary forest, which it was not possible with the single use of backscatter.
6. Given the increasing power of modern computers, feature selection by exhaustive search, based on overall accuracy, is becoming feasible for moderate dimensionality.
7. Joint use of other radar sources can improve mapping accuracy.
8. Matched filtering provides a good radar texture extraction method, either by autorregressive modeling or whitening filters constructed by principal components of Laws filters.

It is clear the usefulness of L-band data as an information source for tropical environment understanding. Given also the experience gathered using SIR-C polarimetric L-band data for limited areas, a considerable success for the forthcoming ALOS system is expected.

6 Acknowledgements.

The authors want to thank NASDA and RESTEC for supplying all high resolution data that made this research possible and Jet Propulsion Laboratory. The research was also partially funded by grants from Finep/PPG7 0808/95 and 0816/95, FAPESP 1997/0943-8 and CNPq 301 400/91-1, 300 927/92-4, 300 677/91-0, 381 246/97-3 and 300 209/94-0.

7 References.

- Costa, M.P.F.; Novo, E.M.L.M.; Mitsuo Ii, F.; Mantovani, J.E.; Ballester, M.V.; Ahern, F. Classification of floodplain habitats (Lago Grande, Brazilian Amazon) with Radarsat and JERS-1 data. In: **International Symposium Geomatics in the Era of Radarsat (GERS'97)**. Ottawa, Canada, 24-30 May, 1997. *Proceedings*.
- Dutra, L. *Classificação de Texturas usando Modelos ARMA e Distâncias da Função de Autocorrelação*. (PhD thesis in Computer Science). Instituto Nacional de Pesquisas Espaciais, São José dos Campos, April 1990, 162 p. (INPE-5067-TDL/406).
- Dutra, L.V.; Huber, R. ; Hernandez F.; P.; Primary Forest and Land Cover Contextual Classification Using JERS-1 data in Amazonia, Brazil. In: **Intern Geosc. And Remote Sensing Symposium. Igarss98**, July, 6-10, 1998, Seattle, EUA
- Frery, A.C.; Müller, H.J.; Yanasse, C.C.F.; Sant'Anna, S.J.S. A model for extremely heterogeneous clutter. *IEEE Trans. Geosc. Rem. Sens.*, 35(3):1-12, May 1997.

- Fukunaga, K. *Introduction to Statistical Pattern Recognition*. Academic Press, 1990.
- Haralick, R.M. Statistical and structural approaches to texture. *Proc. IEEE*, 67(5):786-804, May. 1979.
- Haralick, R.M.; Shanmugam, K.; Dinstein, I. Textural features for image Classification *IEEE Trans. on Systems, Man and Cybernetics*, Vol 3 , No. 6, pp. 610-621, Nov. 1973.
- Huber, R; Dutra, L.V. Feature Selection for ERS-1/2 InSAR Classification: High Dimensionality Case. In: **Intern Geosc. And Remote Sensing Symposium. Igarss98**, July, 6-10, 1998, Seattle, EUA.
- Kay, S.M. *Modern spectral estimation: theory and application*. Prentice Hall, Englewood Cliffs, NJ, 1988. 543p.
- Laws, K.I. *Textured image segmentation. signal and image processing* Institute, PhD Thesis, University of Southern California, Los Angeles, CA, USA, 1980.
- Lee, J.S. Refined filtering of image noise using local statistics. *Computer Graphics and Image Processing*, Vol 15, pp. 380-389, 1981.
- Ma, Z.; Roland L. Redmond,R.L. Tau coefficients for accuracy assessment of classification of remote sensing data. *Photogrammetric Engineering & Remote Sensing*, Vol 61., No. 4, April 1995, pp. 435-439.
- Rennó, C.D.; Freitas, C.C.; Sant'Anna, S.J.S. A system for region image classification based on textural measures. In: **Segunda Jornada Latino-Americana de Sensoriamento Remoto por Radar: Técnicas de Processamento de Imagens**. Santos, São Paulo, set. 1998, *Workshop Proceedings*. ESA, 1998 (ESA SP-434), p. 159-164.
- Ribeiro, M.C.; Alves, D.S.; Soares, J.V.; Yanasse, C.C.F.; Mitsuo Ii, F. Potencialities of using texture measures for mapping land use dynamics based on radar imagery. In: *International Archives of Photogrammetry and Remote Sensing*, Vol. XXXII, Part 7, Budapest, 1998, pp.392-396.
- Rosenqvist, A. *Analysis of the backscatter characteristics of rubber, oil palm and irrigated rice in multiband polarimetric Synthetic Aperture Radar Imagery*. (PhD. Thesis.). Institute of Industrial Science, University of Tokyo. 1997. 114p.
- Sant'Anna, S.J.S.; Yanasse, C.C.F.; Hernandez, P.F.; Kuplich, T.M.; Dutra, L.V.; Frery, A.C.; Santos, P.P. Secondary forest age mapping in Amazônia using multi-temporal Landsat/TM imagery. In: **International Geoscience and Remote Sensing Symposium - Igarss95**, Firenze, Itália, Jul. 04-10, 1995, v.1, pp.323-325.
- Santos, J.R.; Pardi Lacruz, M.S.; Keil, M.; Kux, H.J.H.; Xaud, M.R. Análise da imagem JERS-1 para estimativa da biomassa aérea de florestas tropicais no sudoeste da Amazônia. In: **Simpósio Brasileiro de Sensoriamento Remoto**, 9. Santos, SP., 11-18 set., 1998a. Anais. CDROM.
- Santos, J.R.; Xaud,M.R.; Pardi Lacruz, M.S. Analysis of the backscattering signals of JERS-1 image from savanna and tropical rainforest biomass in Brazilian Amazonia. In: **ISPRS ECO BP'98 - Commission VII**, Budapest, Hungary., 1-4 Sept., 1998b. *Proceedings*. vol. XXXII, part 7., p. 523-526
- Showengerdt, R.A. *Remote Sensing, Models and Methods for Image Processing*. Academic Press, San Diego, CA , 1997, second edition.
- Soares, S.M. *Classificação Textural De Imagens de Radar Por Modelagem Estatística Autorregressiva*. MSc Dissertation on Remote Sensing. Instituto Nacional de Pesquisas Espaciais, São José dos Campos, SP, 1998.
- Soares, S.M.; Dutra, L.V.; Perrela, W. J.; Classificação Textural De Imagens Sar, Por Modelagem Autorregressiva.(SAR Texture Classification By Autorregressive Modelling). In: **Segunda Jornada Latin-Americana De Sensoriamento Remoto Por Radar: Técnicas De Processamento De Imagens**. Santos, São Paulo, set. 1998, Workshop Proceedings. ESA, 1999, (ESA SP-434, pag. 149-152)
- Toutin, T. Multisource data integration with integrated and unified geometric modelling. In: **Sensors and Environment Applications of Remote Sensing**. *Proceedings*. Askne (ed), Balkema, Rotterdam, p. 163-169, 1995.